Synthesis and mesomorphic properties of new organosiloxane chiral calamitic liquid crystals

H. Ocak, B. Karaağaç, H. Akdaş-Kiliç, O. Jeannin, F. Camerel, B. Bilgin Eran

Synthesis and Mesomorphic Properties of New Organosiloxane Chiral Calamitic Liquid Crystals

Hale Ocak[a*], Burcu Karaağaç[a], Huriye Akdaş-Kılıç[a,b], Olivier Jeannin[b], Franck Camerel[b], Belkız Bilgin Eran[a*]

[a]Yildiz Technical University, Department of Chemistry, 34220 Esenler, Istanbul, Turkey
[b]Univ Rennes, CNRS, ISCR - UMR 6226, F-35000 Rennes

*Corresponding Authors: hocak@yildiz.edu.tr, bbilgin@yildiz.edu.tr

Abstract:

A new chiral calamitic compound consisting of a phenyl core which is connected through ester linkers to a benzoate carrying a chiral (*S*)-2-methylbutoxy group at one side and a biphenyl carboxylate with an undecenyloxy chain at other side has been synthesized. Additionally, the siloxane substituted derivatives and a dimer with these two identical chiral calamitics linked by a disiloxane spacer have been obtained via hydrosilylation reaction to study the effect of combining the chiral moiety and siloxane segments within the same structure on liquid crystalline properties. The chiral calamitic compound and derivatives with a siloxane end-group or a siloxane spacer have been characterized using classical spectroscopic methods (^{1}H-NMR, ^{13}C-NMR, ^{29}Si-NMR and MS) and elemental analysis (EA). The liquid crystalline properties of all new compounds were investigated by differential scanning calorimetry, optical polarizing microscopy, X-ray scattering and electro-optic methods. With the introduction of a siloxane end-group to the vinyl-terminated calamitic compound exhibiting enantiotropic chiral nematic phase (N*) and chiral tilted smectic phase (SmC*), the occurrence of stable smectic phase was strongly promoted. In a similar way, the dimer with two identical calamitic mesogens connected by a disiloxane spacer exhibited a wider smectic mesophase interval in addition to the presence of N* mesophase. The new mesogens exhibit a ferroelectric switching with P_S of around 200 nC cm^{-2} in their chiral tilted smectic (SmC*) mesophase range. The transition temperatures of organosiloxanes are considerably lower than that of olefinic precursor.

Keywords: Liquid crystals, chirality, calamitic, organosiloxane, (*S*)-2-methylbutoxy group.

1. Introduction

Liquid crystals which are the unique state of matter have a wide application area such as digital displays, sensors and LCD screens[1,2,3,4,5,6,7]. Structure-mesogenity relationship plays a major role in understanding the properties of liquid crystals. Slight changes in the structural segments can make drastic effects on mesomorphic properties[8,9,10]. The occurence of tilted smectic phases of chiral calamitic liquid crystals are especially important due to their applications in display devices showing fast switching behavior[11]. The materials used frequently in liquid crystal displays are thermotropic liquid crystals with a rod-like shape and exhibit chiral mesophase due to presence of chiral moiety[12,13]. Most of ferroelectric materials consist of a rod-like molecule formed by a rigid core with two flexible terminal chains, at least one of which is chiral[14,15,16,17,18].

In low molar mass organosiloxane[19,20,21,22] liquid-crystal materials, the molecule consists of one or two mesogenic moieties attached via alkyl chains to a short siloxane chain. The siloxane chain has usually less than five repeat units, typically two or three. Introducing siloxane chains into liquid crystal molecules is one of the widely used methods to achieve perfect segregation[23]. Indeed, siloxane groups in a liquid crystal system tend to micro-segregation and cluster the layers leading to dominating smectic phases[24,25].

Bimesogenic dimers, consisting of two mesogenic moieties linked by a flexible short siloxane spacer group, are a very popular subject for their applications; an expected feature is ferroelectricity and anti-ferroelectricity[26] The mesogenic behavior of these mesogenic dimers can be entirely different from their starting monomers, or they can be considered as models for main chain liquid crystal polymers. In general, the mesophase behavior of a mesogenic dimer depends on many factors. In particular, it changes depending on the molecular structure, the size of the mesogenic units and the symmetry of the molecule[27]. Additionally, the ratio between the length of the molecule as well as the length of the terminal chain can strongly affect the structure of the mesophase[28,29].

The aim of this study is the synthesis and characterization of new biphenyl based chiral calamitic mesogens bearing a (*S*)-2-methylbutoxy chiral moiety at one side and a siloxane end chain on the other side as well as the investigation of the effect of combining the chiral moiety and siloxane segments within the same structure on liquid crystalline properties. Additionally, a dimer with the two identical chiral calamitics linked by a disiloxane spacer have been obtained via hydrosilylation reaction. The new chiral calamitic molecules have been characterized using classical spectroscopic methods (^{1}H-NMR, ^{13}C-NMR, ^{29}Si-NMR and MS) and elemental analysis (EA). The mesomorphic properties of all new compounds were determined by

differential scanning calorimetry (DSC), optical polarizing microscopy (POM), X-ray scattering (SAXS) and electro-optic methods (EO).

2. Experimental

2.1 Synthesis, Procedures and Characterization

The synthesis of new biphenyl based chiral calamitic compounds **5-8** consisting of four aromatic benzene rings connected through ester linkers and carrying a flexible chiral chain (*S*)-2-methylbutoxy at one side and an undecenyloxy chain or siloxane end chain at the other was carried out by using previously reported multi-step procedures[30] as seen in Scheme 1.

Compound **1** and **2**[31] were synthesized starting from 4-((*S*)-2-methylbutoxy)benzoic acid[32] which was obtained by the alkylation of ethyl 4-hydroxybenzoate with (*S*)-2-methylbutyltosylate[33], followed by hydrolysis of the ester group with sodium hydroxide solution. 4-((*S*)-2-methylbutoxy)benzoic acid was reacted with *p*-benzyloxyphenol using N,N'-dicyclohexylcarbodiimide (DCC) and 4-(dimethylamino)pyridine (DMAP)[34] followed by the hydrogenolytic debenzylation with H_2 gas, %10 Pd/C in THF to yield compound **2** which was purified by column chromatography on silica gel using dichloromethane as eluent and recrystallized from hexane.

The synthesis of the other key intermediate, 4'-(10-undecen-1-yloxy)-4-biphenylcarboxylic acid (**4**)[35] was carried out by the esterification of commercially available ethyl 4'-hydroxy-4-biphenyl carboxylate with the 11-Bromo-1-undecene using K_2CO_3 as base in dry 2-butanone. The obtained compound **3**[35] was hydrolyzed using 10 N sodium hydroxide solution in ethanol to yield target biphenylcarboxylic acid (**4**) which was purified by recrystallization from ethanol. The spectroscopic data (^{1}H-, ^{13}C-NMR and MS (EI)) of the compounds **1**-**4** are given in the ESI.

For the preparation of the vinyl-terminated calamitic compound (**5**), 4'-(10-undecen-1-yloxy)-4-biphenylcarboxylic acid (**4**)[35] was reacted with 4-hydroxyphenyl 4-((*S*)-2-methylbutoxy)benzoate (**2**)[31] via Steglich esterification method. The unsaturated compound **5** was reacted with 1*H*-heptamethyltrisiloxane or 1*H*,3*H*-tetramethyldisiloxane by a hydrosilylation reaction[36,37] using Karstedt's catalyst to yield the siloxanes **6** and **7** respectively. Finally, chiral siloxane-based dimer **8** was obtained from compound **7** by using the same conditions. All target compounds were fully characterized using classical spectroscopic methods (see *ESI*).

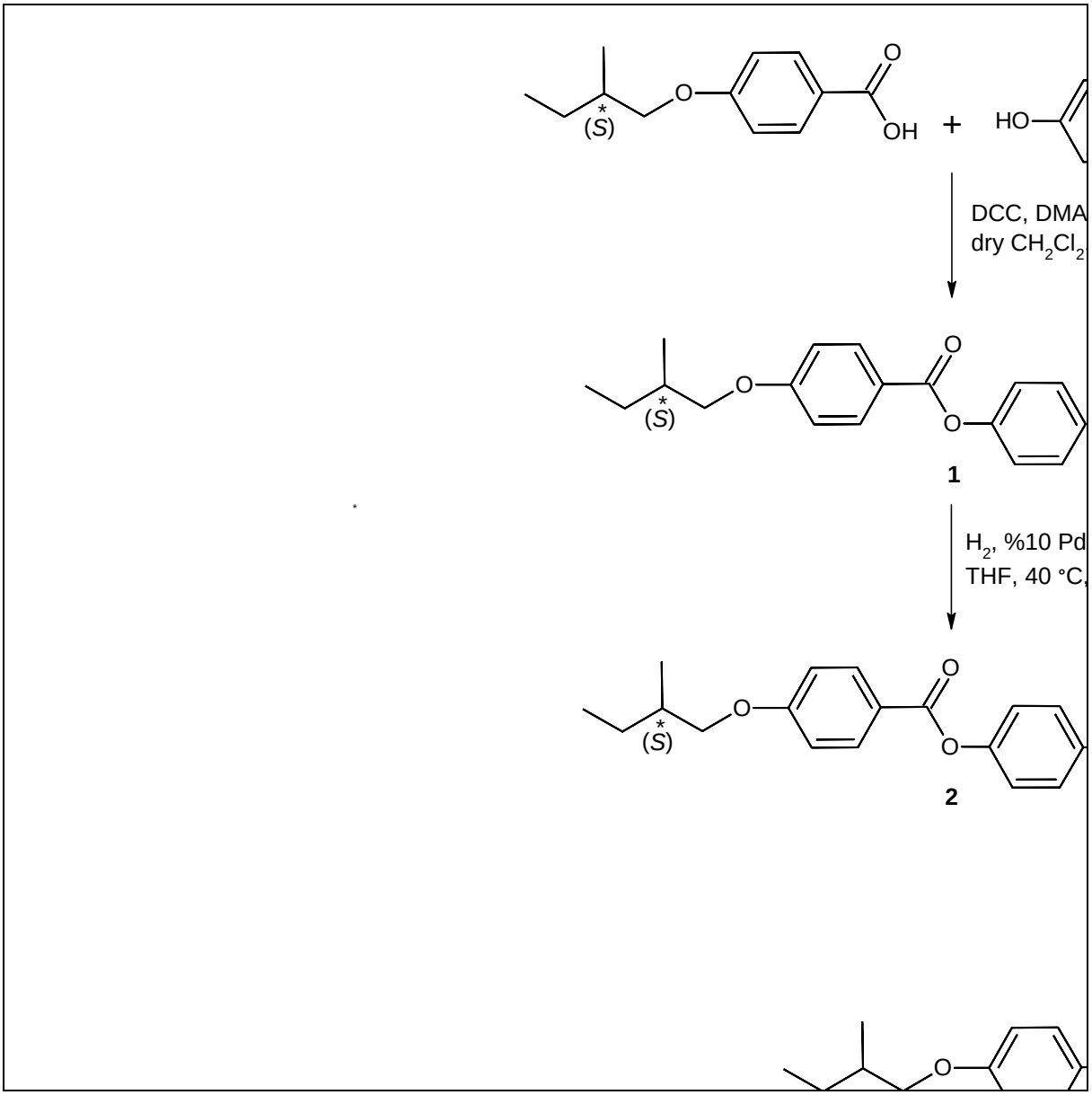

Scheme 1. Synthesis of the compounds **1-8**.

Compound 5

General procedure: 4 mmol (1.20 g) of compound **2** and 4 mmol (1.47 g) of compound **4** were dissolved in 50 mL of dry dichloromethane under argon atmosphere at room temperature. After the addition of 4 mmol (0.77 g) of N-(3-Dimethylaminopropyl)-N′-ethylcarbodiimide hydrochloride and 0.8 mmol (0.098 g) of 4-(dimethylamino)pyridine (DMAP), the reaction mixture was stirred at room temperature for 24 hours and the reaction was monitored by TLC ($CHCl_3$). The filtration of the reaction mixture over silica gel to remove the catalyst residue which was performed, and the silica gel was washed with several portions of CH_2Cl_2. The

combined organic phases were evaporated under vacuum and the product was purified by column chromatography (silica gel 60, $CHCl_3$) and recrystallized with ethanol.

4-((*S*)-2-Methylbutoxy)-benzoyloxyphenyl 4-(10-undecen-1-yloxy)biphenyl-4'-carboxylate (5) ($C_{42}H_{48}O_6$; 649.83 g/mol): Yield, 75 %; colorless crystals. **^{1}H NMR** (500 MHz, $CDCl_3$): δ (ppm) = 8.22 (d, *J* ≈ 8.5 Hz, 2Ar-C*H*), 8.13 (d, *J* ≈ 8.8 Hz, 2Ar-C*H*), 7.68 (d, *J* ≈ 8.5 Hz, 2Ar-C*H*), 7.58 (d, *J* ≈ 8.8 Hz, 2Ar-C*H*), 7.26 (s, broad, 4Ar-C*H*), 7.00 (d, *J* ≈ 8.8 Hz, 2Ar-C*H*), 6.97 (d, *J* ≈ 8.8 Hz, 2Ar-C*H*), 5.81-5.76 (m, 1H, CH_2=C*H*), 5.00-4.90 (m, 2H, CH_2=CH), 4.00 (t, *J* ≈ 6.5 Hz, 2H, OCH_2), 3.90, 3.82 (2dd, each, J_1 ≈ 9.1 Hz and J_2 ≈ 6.0 Hz, 2H, OCH_2), 2.05-2.01 (m, 2H, CH_2), 1.94-1.76 (m, 3H, C*H*, CH_2), 1.61-1.52, 1.47-1.24 (2m, 14H, 7CH_2), 1.03 (d, *J* ≈ 6.6 Hz, 3H, CH_3), 0.96 (t, *J* ≈ 7.5 Hz, 3H, CH_3). **^{13}C NMR** (125 MHz, $CDCl_3$): δ (ppm) = 164.86, 164.67 (*C*O), 163.66, 159.50, 148.45, 148.26, 145.97, 131.92, 127.34, 121.00 (Ar-*C*), 139.08 (CH_2=*C*H), 132.20, 130.64, 128.30, 126.54, 122.62, 122.50, 115.00, 114.33 (Ar-*C*H), 114.06 (CH=*C*H_2), 73.18, 68.23 (O*C*H_2), 34.75 (*C*H), 33.87, 29.59, 29.50, 29.46, 29.36, 29.20, 29.03, 26.21, 26.14 (*C*H_2), 16.59, 11.39 (*C*H_3). **$C_{42}H_{48}O_6$** (649.83); Anal. Calc. (%): C, 77.75; H, 7.46. Found (%): C, 77.50; H, 7.45. **MS (ESI) (+): m/z (%) =** 649 (13) [M^+], 349 (100) [M^+-$C_{18}H_{19}O_4$], 191 (98) [$C_{12}H_{15}O_2$], 121 (98) [$C_7H_5O_2$].

Compound 6 and 7

General procedure: 2 mmol (1.30 g) of compound **5** and 2 mmol of 1,1,1,3,3,5,5-heptamethyltrisiloxane (0.44 g) or 1,1,3,3-tetramethyldisiloxane (0.27 g) were dissolved in 40 mL of dry toluene under argon atmosphere. After the addition of catalytic amount of Karstedt's catalyst (Platinum(0)-1,3-divinyl-1,1,3,3-tetramethyldisiloxane complex solution in xylene), the reaction mixture was stirred at 40 °C for two days and the reaction was monitored by TLC (H: EA/10:1). The reaction mixture was filtered over silica gel and washed with toluene. The combined organic phases were evaporated under vacuum and the product was purified by column chromatography (silica gel 60, H: EA/5:1) and recrystallized with ethanol.

4-((*S*)-2-Methylbutoxy)benzoyloxyphenyl 4-[11-(1,1,1,3,3,5,5-hexamethyltrisiloxane)undec-1-yloxy]biphenyl-4'-carboxylate (6) ($C_{49}H_{70}O_8Si_3$, 871.34 g/mol): Yield, 40 %; colorless crystals. **^{1}H NMR** (500 MHz, $CDCl_3$): δ (ppm) = 8.15 (d, *J* ≈ 8.5 Hz, 2Ar-C*H*), 8.06 (d, *J* ≈ 8.9 Hz, 2Ar-C*H*), 7.61 (d, *J* ≈ 8.5 Hz, 2Ar-C*H*), 7.51 (d, *J* ≈ 8.8 Hz, 2Ar-C*H*), 7.20 (s, broad, 4Ar-C*H*), 6.92 (d, *J* ≈ 8.8 Hz, 2Ar-C*H*), 6.90 (d, *J* ≈ 8.9 Hz, 2Ar-C*H*), 3.93 (t, *J* ≈ 6.6 Hz, 2H, OCH_2), 3.83, 3.75 (2dd, each, J_1 ≈ 9.1 Hz and J_2 ≈ 6.0 Hz, 2H,

OCH_2), 1.86-1.79 (m, 1H, C*H*), 1.76-1.70 (m, 2H, OCH_2CH_2), 1.55-1.44, 1.42-1.36 (2m, 4H, 2CH_2), 1.28-1.12 (m, 14H, 7CH_2), 0.96 (d, $J \approx 6.8$ Hz, 3H, CH_3), 0.89 (t, $J \approx 7.4$ Hz, 3H, CH_3), 0.44 (t, $J \approx 7.3$ Hz, 2H, SiCH_2), 0.00 (s, 9H, 3CH_3Si), -0.03 (s, 6H, 2CH_3Si), -0.07 (s, 6H, 2CH_3Si). **^{13}C NMR** (125 MHz, $CDCl_3$): δ (ppm) = 165.02, 164.83 (*C*O), 163.76, 159.60, 148.52, 148.33, 146.05, 131.95, 127.35, 121.35 (Ar-*C*), 132.28, 130.72, 128.37, 126.60, 122.70, 122.58, 114.99, 114.34 (Ar-*C*H), 73.12, 68.18 (OCH_2), 34.64 (*C*H), 33.44, 29.69, 29.58, 29.41, 29.39, 29.35, 29.26, 26.09, 26.05, 23.22 (CH_2), 18.29 (SiCH_2), 16.48, 11.29 (2CH_3), 1.80, 1.27, 1.01 (7CH_3Si). **^{29}Si NMR** (100 MHz, $CDCl_3$): δ (ppm) = 7.42, 6.97, -21.13. **$C_{49}H_{70}O_8Si_3$** (871.34); Anal. Calc. (%): C, 67.54; H, 8.10. Found (%): C, 67.25; H, 7.90. **MS (ESI) (+): m/z (%) =** 867 (9.1) [M^+], 571 (99) [M^+-$C_{18}H_{19}O_4$], 221 (73) [M^+-$C_{24}H_{30}O_2$], 191 (100) [M^+-CH_2O], 120 (99) [$C_7H_4O_2$].

4-((*S*)-2-Methylbutoxy)benzoyloxyphenyl 4-[11-(1,1,3,3-tetramethyldisiloxane) undec-1-yloxy]biphenyl-4'-carboxylate (7) ($C_{46}H_{62}O_7Si_2$, 783.16 g/mol): Yield, 20 %; colorless crystals. **^{1}H NMR** (500 MHz, $CDCl_3$): δ (ppm) = 8.22 (d, $J \approx 8.5$ Hz, 2Ar-C*H*), 8.13 (d, $J \approx 8.9$ Hz, 2Ar-C*H*), 7.68 (d, $J \approx 8.5$ Hz, 2Ar-C*H*), 7.58 (d, $J \approx 8.7$ Hz, 2Ar-C*H*), 7.26 (s broad, 4Ar-C*H*), 6.97 (d, $J \approx 8.9$ Hz, 2Ar-C*H*), 6.95 (d, $J \approx 8.9$ Hz, 2Ar-C*H*), 4.68-4.65 (m, Si*H*), 4.00 (t, $J \approx 6.5$ Hz, 2H, OCH_2), 3.90, 3.82 (2dd, each, $J_1 \approx 9.1$ Hz and $J_2 \approx 6.0$ Hz, 2H, OCH_2), 1.94-1.76 (m, 3H, C*H*, CH_2), 1.63-1.24 (m, 18H, 9CH_2), 1.03 (d, $J \approx 6.8$ Hz, 3H, CH_3), 0.95 (t, $J \approx 7.4$ Hz, 3H, CH_3), 0.51 (t, $J \approx 6.7$ Hz, 2H, SiCH_2), 0.17 – (-0.01) (m, 12H, 4SiCH_3). **^{13}C NMR** (125 MHz, $CDCl_3$): δ (ppm) = 165.01, 164.82 (*C*O), 163.70, 159.53, 148.45, 148.25, 145.99, 131.86, 127.25, 121.24 (Ar-*C*), 132.24, 130.68, 128.33, 126.55, 122.68, 122.56, 114.91, 114.27 (Ar-*C*H), 73.04, 68.09 (OCH_2), 34.56 (*C*H), 33.34, 29.58, 29.52, 29.36, 29.31, 29.19, 26.02, 23.12, 18.06 (CH_2), 16.43, 11.26 (CH_3), 0.86, -0.01 (SiCH_3). **$C_{46}H_{62}O_7Si_2$** (783.16); Anal. Calc. (%): C, 70.55; H, 7.98. Found (%): C, 70.27; H, 7.71. **MS (ESI) (+): m/z (%) =** 782 (6) [M^+], 483 (29) [M^+-$C_{18}H_{19}O_4$], 329 (33) [$C_{11}H_{22}$], 191 (98) [$C_{12}H_{15}O_2$], 121 (86) [$C_7H_5O_2$].

Compound 8

General procedure: 2 mmol (1.57 g) of compound **7** and 2 mmol (0.27 g) of 1,1,3,3-tetramethyldisiloxane were dissolved in 40 mL of dry toluene under argon atmosphere. After the addition of catalytic amount of Karstedt's catalyst (Platinum(0)-1,3-divinyl-1,1,3,3-tetramethyldisiloxane complex solution in xylene), the reaction mixture was stirred at 40 °C for two days and the reaction was monitored by TLC (H: EA/10:1). The reaction mixture was

filtered over silica gel and washed with toluene. The combined organic phases were evaporated under vacuum and the product was purified by column chromatography (silica gel 60, H: EA/5:1) and recrystallized with ethanol.

1,3-Di[4-(11-undec-1-yloxy)biphenyl]-4'-carboxylic acid 4-((*S*)-2-Methylbutoxy) benzoyloxyphenyl ester] 1,1,3,3-tetramethyldisiloxane (8) ($C_{88}H_{110}O_{13}Si_2$, 1432.0 g/mol): Yield, 20 %; colorless crystals. **^{1}H NMR** (500 MHz, $CDCl_3$): δ (ppm) = 8.17 (d, $J \approx 8.5$ Hz, 4H, Ar-C*H*), 8.08 (d, $J \approx 8.9$ Hz, 4H, Ar-C*H*), 7.63 (d, $J \approx 8.5$ Hz, 4H, Ar-C*H*), 7.53 (d, $J \approx 8.8$ Hz, 4H, Ar-C*H*), 7.21 (s broad, 8H, Ar-C*H*), 6.94 (d, $J \approx 8.8$ Hz, 4H, Ar-C*H*), 6.92 (d, $J \approx 8.8$ Hz, 4H, Ar-C*H*), 3.95 (t, $J \approx 6.5$ Hz, 4H, 2OCH_2), 3.84, 3.76 (2dd, each $J_1 \approx 9.0$ Hz and $J_2 \approx 6.0$ Hz, 4H, 2OCH_2), 1.88-1.72 (m, 6H, 2C*H*, *2*CH_2), 1.54-1.20 (m, 36H, 18CH_2), 0.98 (d, $J \approx 6.7$ Hz, 6H, 2CH_3), 0.90 (t, $J \approx 7.4$ Hz, 6H, 2CH_3), 0.82 (t, $J \approx 6.9$ Hz 4H, 2SiCH_2), 0.10 - (-0.07) (m, 12H, 4SiCH_3). **^{13}C NMR** (125 MHz, $CDCl_3$): δ (ppm) = 165.08. 164.89 (*C*O), 163.77, 159.59, 148.51, 148.32, 146.06, 131.93, 127.31, 121.30 (Ar-*C*), 132.31, 130.75, 128.40, 126.62, 122.75, 122.63, 114.98, 114.34 (Ar-*C*H), 73.11, 68.16 (O*C*H_2), 34.63 (*C*H), 31.92, 29.61, 29.59, 29.53, 29.40, 29.35, 29.24, 26.08, 26.04, 22.70, 16.49 (*C*H_2), 14.14, 11.32 (*C*H_3), 0.00 (Si*C*H_3).

3. Results and Discussions

3.1 Optical investigation and DSC Measurements

The liquid crystal properties of the intermediates **3** and **4**[35], the vinyl-terminated calamitic compound **5** and siloxane-based biphenyl chiral calamitic compounds **6-8** were investigated by using optical polarizing microscope (POM) and differential scanning calorimeter (DSC). The phase transitions temperatures and corresponding transition enthalpies of the compounds **5-8** as observed on heating and cooling cycles are given in Table 1 as well as Table S1 for intermediates **3** and **4**. The peak temperatures are given in degree Celsius and the numbers in parentheses indicate the transition enthalpy (Δ*H*) (see Table 1 and Table S1 in ESI).

The heating runs of the DSC curves recorded for the biphenyl ester **3** show four transitions which were in a phase sequence Cr - SmX_1 - SmX_2 - SmA – Iso (Table S1, Fig. S25 in ESI). Similarly, four transitions, which correspond to Iso - SmA - SmX_2 - SmX_1 - Cr phase sequence, were observed during cooling from the isotropic state and a fan-shaped texture started to appear below 97 °C under POM (see Fig.1a). On further cooling, SmX_2 and SmX_1 mesophases

occurred at 84 °C and 71.7 °C respectively (see Fig. S26 in *ESI*). Besides, the acid-end analog **4** exhibits smectic C mesophase within a phase sequence Cr - SmC - Iso on heating as well as reverse phase transition sequence on cooling. The SmC phase appeared with a Schlieren texture obtained on cooling (see Fig.1b). While SmA mesophase was observed in a narrow temperature range in compound **3**, the acid-end analog **4**, resulted in the smectic C phase with a wider mesomorphic temperature range. The results of X-ray scattering experiments (SAXS) of compounds **3** and **4** were discussed in ESI (see Fig. S27, S28 and Table S2).

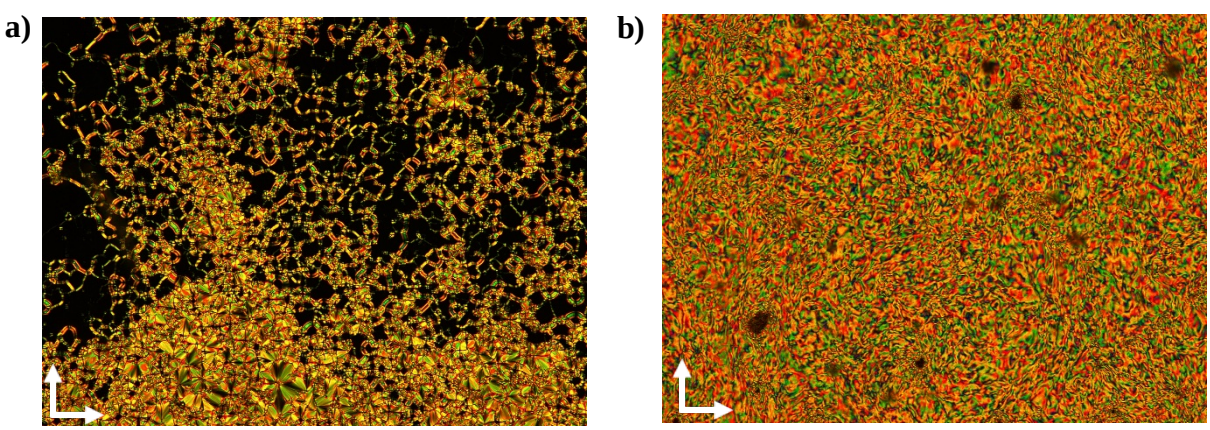

Figure 1. Optical textures of mesophases as observed between crossed polarizers (indicated by arrows) in ordinary glassplates on cooling; (a) fan-shaped texture of SmA mesophase of compound **3** obtained at T = 93 °C; (b) Schlieren texture of SmC mesophase of compound **4** obtained at T = 179 °C.

On heating DSC thermogram of compound **5**, three transitions which correspond to a phase transition sequence of crystal Cr - SmC* - N* - Iso were detected (see Table 1, see Fig. 2). One exothermic peak observed around 90 °C on the heating thermogram which indicates that the phase isolated below 110 °C upon cooling is metastable and that this phase recrystallizes upon heating. The high energy peak observed at 142.2 °C on the heating thermogram is associated to the transition of the crystalline phase into a liquid crystalline phase. Above 150 °C, compound **5** shows two perfectly reversible phase transitions centered at 191.3 and 271.6 °C. On cooling from isotropic phase, the DSC curve of this compound shows three distinct phase transitions. Compound **5** exhibits an enantiotropic tilted chiral smectic (SmC*) mesophase which was identified with a stripe pattern and an enantiotropic chiral nematic mesophase (N*) with a typical oily streaks texture (see Fig. 3a and 3b).

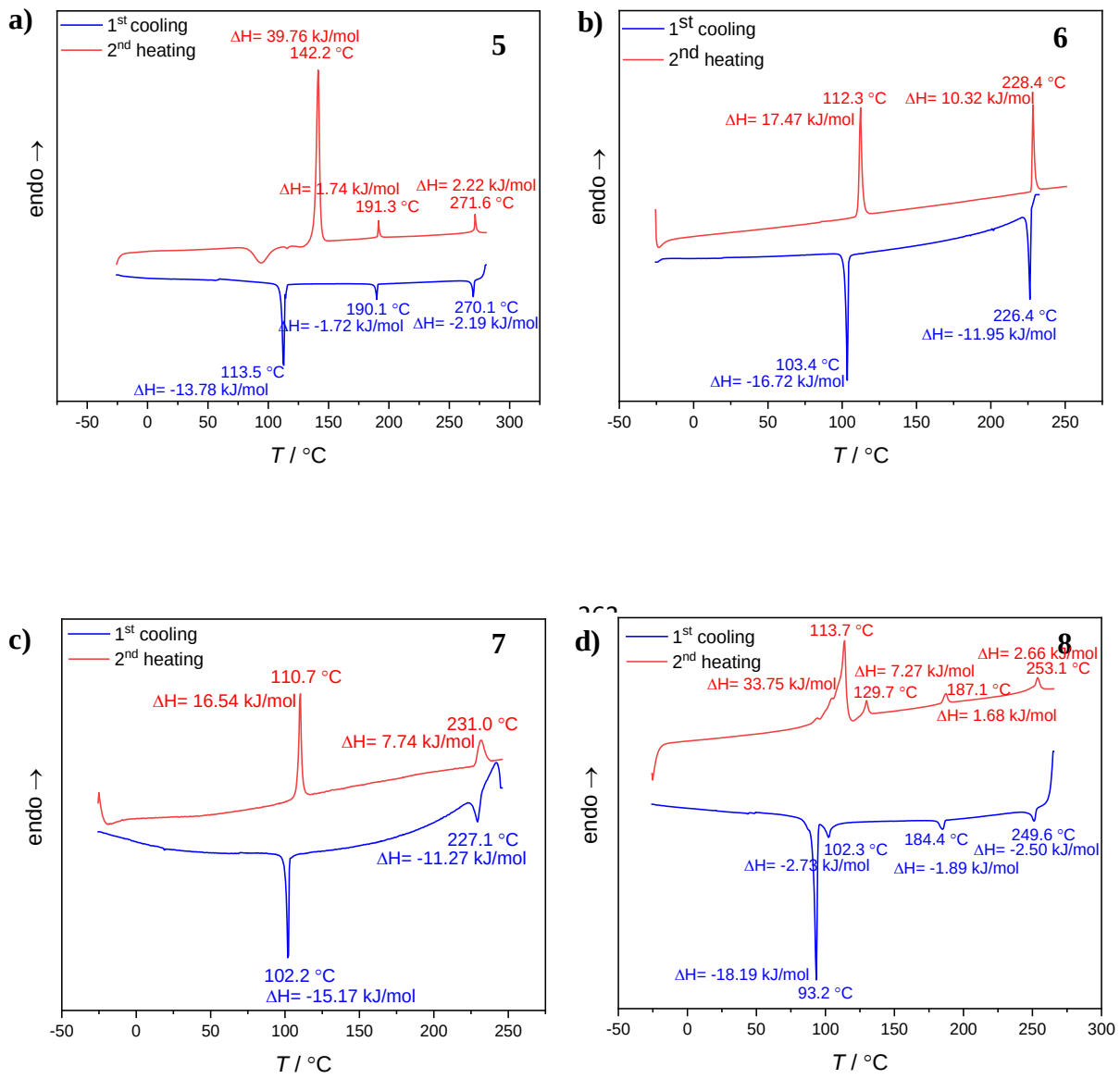

Figure 2. DSC thermograms of compounds **5 - 8** on 2nd heating and 1st cooling (10 °C.min^{-1}).

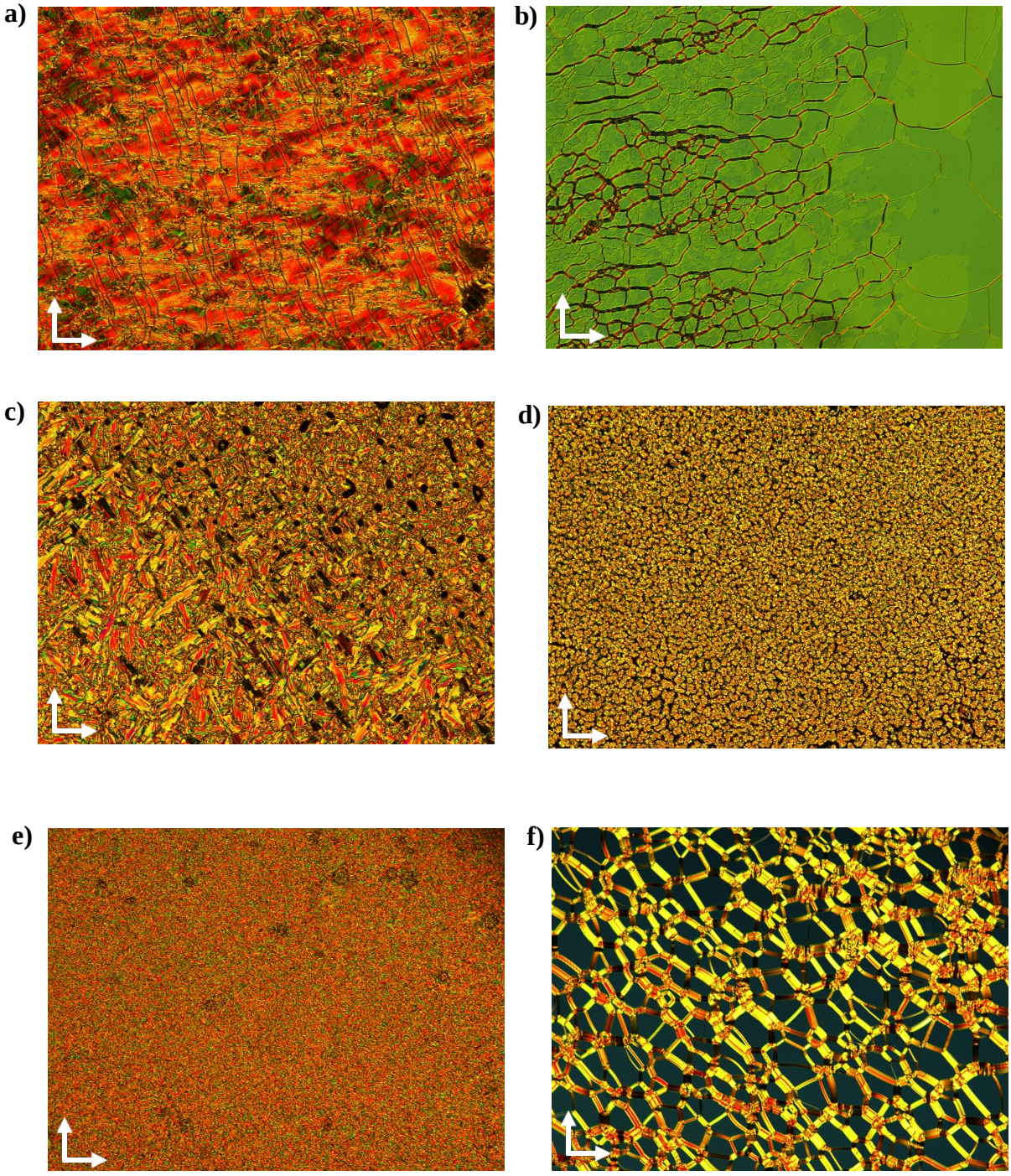

Figure 3. Optical textures of mesophases of compounds **5**-**8** as observed between crossed polarizers (indicated by arrows) in a 10 μm PI coated ITO cell providing planar alignment on cooling; (a) texture of SmC* mesophase of compound **5** at T = 162 °C; (b) Oily-streak texture of N* mesophase of compound **5** at T = 233 °C; (c) texture of SmC* mesophase of compound **6** at T = 133 °C; (d) texture of SmC* mesophase of compound **7** at 160 °C; (e) texture of SmC* mesophase of compound **8** at 182 °C; (f) Oily-streak texture of N* mesophase of compound **8** at 246 °C.

Table 1. Mesophases, phase transition temperatures and associated enthalpies of the compounds **5**-**8** on heating (H→) and cooling (C→).

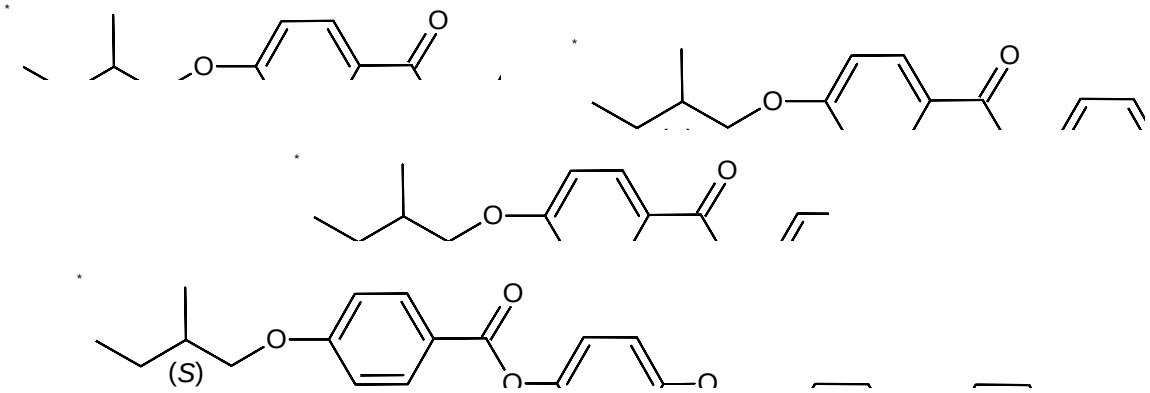

Comp.	T / °C [ΔH kJ/mol]
5	**H**→ Cr 142.2 [*39.76*] SmC* 191.3 [*1.74*] N* 271.6 [*2.22*] Iso **C**→ Iso 270.1 [*-2.19*] N* 190.1 [*-1.72*] SmC* 113.5 [*-13.78*] Cr
6	**H**→ Cr 112.3 [*17.47*] SmC* 228.4 [*10.32*] Iso **C**→ Iso 226.4 [*-11.95*] SmC* 103.4 [*-16.72*] Cr
7	**H**→ Cr 110.7 [*16.54*] SmC* 231.0 [*7.74*] Iso **C**→ Iso 227.1 [*-11.27*] SmC* 102.2 [*-15.17*] Cr
8	**H**→ Cr_1 113.7 [*33.75*] Cr_2 129.7 [*7.27*] SmC* 187.1 [*1.68*] N* 253.1 [*2.66*] Iso **C**→ Iso 249.6 [*-2.50*] N* 184.4 [*-1.89*] SmC* 102.3 [*-2.73*] Cr_2 93.2 [*-18.19*] Cr_1

[a] NETZSCH DSC 200 F3; enthalpy values in italics in brackets taken from the 2nd heating and 1st cooling scans at a rate of 10 °C min^{-1}; Abbreviations: Cr = crystalline, SmC* = chiral tilted smectic phase, N*= chiral nematic phase, Iso = isotropic liquid phase.

The DSC thermograms of compound **6**, a chiral calamitic ester carrying a bulk trisiloxane end chain shows two perfectly reversible endotherms for a phase transition sequence of Cr - SmC* - Iso and two exotherms for the reverse phase transition sequence. SmC* phase was detected with a characteristic fingerprint texture by optical polarizing microscope (POM) observation (see Fig. 3c). As reported studies on liquid crystals containing siloxane[38], the incorporation of bulk siloxane units into the mesogenic structure leads to the stratification by the effect of microsegregation. This effect gives rise to the suppression of the chiral nematic (N*) phase in the siloxane material and conduct to the formation of smectic phases. Additionally, a striking decrease on the clearing point was observed by the introduction of the siloxane unit as compared to compound **5**.

The mesogenic properties of bulk disiloxane based chiral calamitic ester **7** are similar to that of compound **6** (see Table 1 and Fig.3d). Compound **7** exhibits a reversible phase transition

sequence of Cr - SmC*- Iso appearing with two endotherms as well as two exotherms on DSC heating curves.

The dimerization of the calamitic molecule **7** via siloxane bridge leads to the occurrence of the polymorphism (see Table 1, Fig. 3e and 3f). The chiral nematic phase (N*) which was observed for olefinic-terminated mesogen **5** also appeared on both heating and cooling process with compound **8**. Indeed, compound **8** shows four reversible thermal transitions at 113.7, 129.7, 187.1 and 253.1 °C on the DSC heating thermogram and the reverse phase transitions was observed on cooling from isotropic phase. Various models for siloxane bridged dimer structures have been proposed in literature concerning the arrangement of dimer derivatives in the mesophase. Each dimer molecule has a unique shape, for example, in the study of Kaneko and co-workers, phenyl-ester based dimer molecules have shown smectic A mesophase and therefore, dimer molecules have been modelled to be arranged on top of each other[39]. On the other hand, Coles and colleagues reported that the biphenyl-ester based molecules which show a chiral smectic C* mesophase with ferroelectric and antiferroelectric behavior related to the order and angles of the molecules[40].

3.2 XRD investigation of compounds 5 - 8

Compound 5

The SAXS patterns measured upon heating confirms that the presence of a crystal to crystal phase transition between 100 °C and 140 °C (Figure 4). The SAXS patterns, obtained between 140 °C and 190 °C, are characteristic of a liquid crystalline smectic phase (see Table 2). In fact the SAXS patterns display two sharp peaks in the small angle region which can be indexed as the two first reflections of a lamellar phase. Additionally, the broad peak centered at 4.6 Å, associated to the molten state of the carbon chains, is observed. The size of the molecule, in its fully extended form, was estimated to be around ~40 Å. Based on POM observations and the SAXS measurements (d<l), it can be deduced that the mesophase is constituted of monolayers of tilted molecules, i.e. smectic C* phase. Above 190 °C, the entering into the nematic phase is characterized by a broadening of the 1st order diffraction peak and a strong decrease of the intensity together with the disappearance of the second order reflection. The decrease of the intensity and the broadening of peak is continuous up to the isotropic phase at 280 °C.

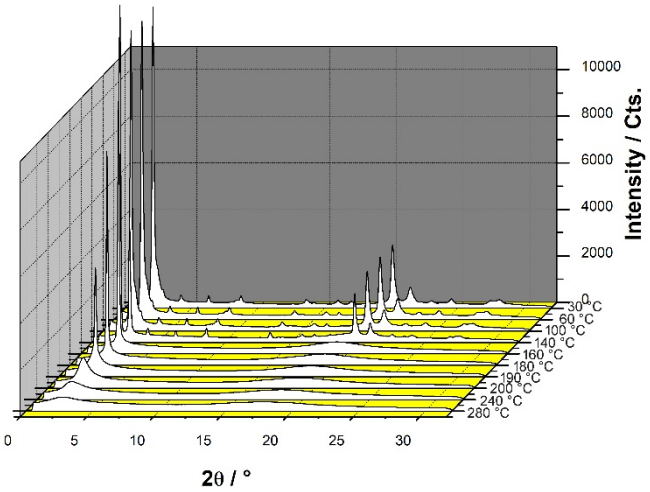

Figure 4. SAXS patterns recorded on compound **5** upon heating.

Table 2 Crystallographic data of compounds **5-8**.

Comp.	T/ °C	Phase	d_{meas}/Å	00l/hk	Lattice parameters
5	180 °C	SmC*	31.09 15.59 4.60	001 002 h_{ch}	*d* = 31.1 Å
6	150 °C	SmC*	39.62 19.76 7.00 4.60	001 002 h'_{stack} h_{Ch}	*d* = 39.6 Å
7	120 °C	SmC*	36.68 18.40 12.23 6.80 4.56	001 002 003 h'_{stack} h_{ch}	*d* = 36.7 Å
8	170 °C	SmC*	34.84 8.25 4.64	001 h'_{stack} h_{ch}	*d* = 34.8 Å
	240 °C	N*	33.82 8.16 4.57	-	-

Compound 6

Compound **6** displays two sharp and reversible thermal transitions centered at 108 °C and 227 °C. All the SAXS patterns obtained between 230 °C and 110 °C display a sharp and intense (001) reflection together with a weak second order reflection (002) (see Fig. 5, Table 2). The broad halo centered around 4.60 Å, confirm the liquid crystalline nature of the phase. The broad halo also observed around 12.6° in 2θ (~7 Å) indicates a head to tail organization of pi-stacked

molecules within the layers. A head to tail organization of the molecules within the layers also allows to accommodate the bulkier siloxane fragments. The length of the molecule in a fully extended conformation was estimated around 48 Å, implying a tilt angle of 34° of the molecules inside the layers. A model of organization of molecule **6** in the smectic phase is presented in Fig. 6. Below 110 °C, the SAXS patterns displays several sharp peaks over the whole 2θ range explored and clearly highlight the crystallization of the compound.

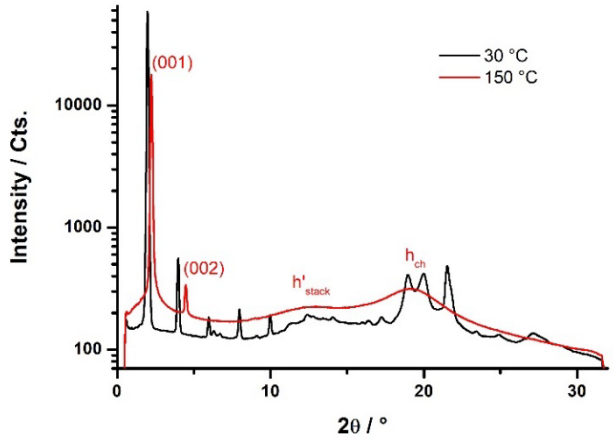

Figure 5. SAXS patterns of compound **6** recorded at 150 °C and 30 °C upon cooling (1st cooling).

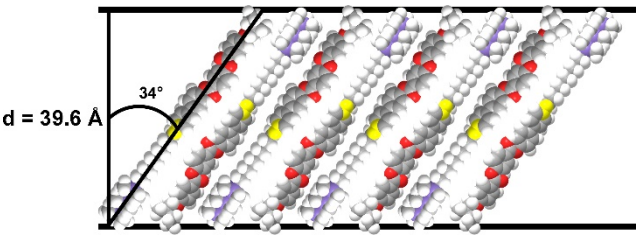

Figure 6. Model of the layer organization at 150 °C of compound **6** in the smectic C* mesophase.

Compound 7

The DSC traces of compound **7** display two reversible thermal transition centered at 106 °C and 229 °C. Above 229 °C, the compound is in an isotropic state and the SAXS patterns display two broad halos centered at 38.7 and 5.16 Å. Between 229 °C and 106 °C, the SAXS patterns obtained are typical of a smectic phase with three sharp peaks in the small angle region which can be indexed as the (001), (002) and (003) reflections of a lamellar phase together with a broad peak (h_{ch}) in the high angle region arising from the carbon chains in a molten state (see Fig. 7, Table 2). The lamellar period measured at 120 °C is 36.7 Å and is almost insensitive to

the temperature increase up to the isotropic phase. A weak and broad halo (h'_{stack}) can also be distinguished around 13° in 2θ and is here also attributed to head to tail arrangement of the molecules within the layers. Based on the length of the molecule in its fully extended form (l ~ 45 Å) and the layer spacing, a molecular tilt angle of 35° can be estimated. The molecular organization of **7** inside the layers should be really close to the one observed with compound **6** (see Fig. 6). The use of a shorter terminal 1,1,3,3-tetramethyldisiloxane fragment in place of a heptamethyltrisiloxane fragment induces a slight contraction of the lamellar period without affecting the domain of existence of the smectic C* phase. Finally, the SAXS patterns obtained below 106 °C confirm the crystallization of the compound at low temperatures and several additional sharp peaks are observed in the high and low angle regions.

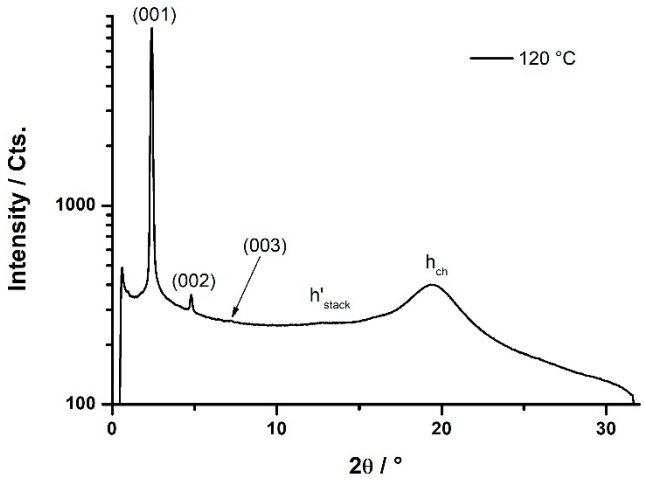

Figure 7. SAXS patterns of compound **7** recorded at 120 °C (1st cooling).

Compound 8

All the SAXS patterns, recorded below 120 °C, are characteristic of a crystalline phase and display several sharp peaks in the small and high angle regions (see Fig. 8). A clear crystal-to-crystal phase transition was detected between 80 °C and 110 °C. Thus, the high energy transition detected around 103 °C is attributed to a crystal-to-crystal phase transition. Upon further heating above 120 °C, the compound entered into a liquid crystalline phase. The SAXS patterns obtained between 120 and 180 °C, display only one sharp peak around 2.5° in 2θ in the small angle region and two broad peaks centered at 10.8° and 19° in 2θ in the high angle region. These SAXS patterns are characteristic of a liquid crystalline compound with molecules organized within molten carbon chains. The broad peak centered at 8.16 Å is indicative of an alternated stacking of ~4Å, which could correspond to the thickness of the molecule in flat configuration. Based on POM observations, this liquid crystalline phase was found to be a

smectic C* mesophase. The lamellar period measured at 170 °C is 34.8 Å (see Table 2) and the length of the molecule in its fully extended form was estimated to be around ~85 Å. Thus, to be able to fit into the lamella, the molecule should be bended around the central Si-O-Si bond with the two aromatic arms facing each other. In addition, since the length of one extended arm was estimated around ~41 Å and the bended molecules should be tilted by ~ 32 ° inside the lamella. A model of the organization of the molecule of compound **8** is proposed in Figure 9. Interestingly, above 170 °C, the diffraction peak in the small angle region start to decrease in intensity and to broaden up to 220 °C and suddenly, the peak become really intense and sharp in the new liquid crystalline phase reached. From POM observations, this high temperature LC phase was identified as a chiral nematic phase (N*). The decrease of the peak intensity and its broadening in the smectic phase can be explained by a gradual unbending of the molecules which finally adopt a fully extended conformation into the nematic phase which appears at higher temperature. Finally, the SAXS patterns recorded above 250 °C confirmed that the highest phase is an isotropic phase and only broad halos of weak intensity have been detected over the whole 2θ range explored. Interestingly, all the compounds carrying a siloxane fragment on one hand and a chiral carbon chain on the other hand display a smectic C* mesophase over large temperature ranges and only when the two aromatic cores where connected through a short siloxane fragment, an additional high temperature phase N* has been detected. As reported by Coles and co-workers[40], the microsegregation of the aromatic, paraffinic and siloxane moieties gives rise to the formation of smectic phase and the suppression of the chiral nematic phase in siloxane-containing mono-structured molecules.

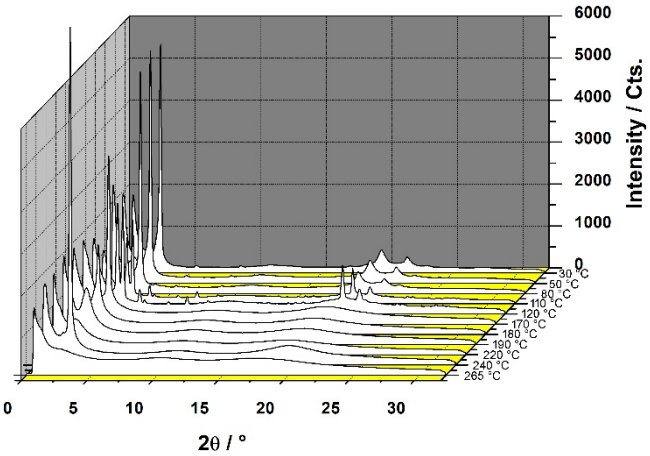

Figure 8. SAXS patterns recorded on compound **8** upon heating.

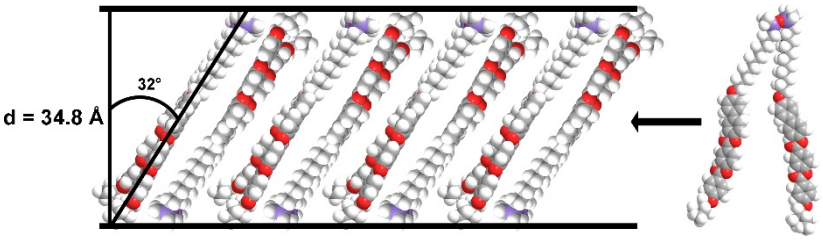

Figure 9. Proposed model for the organization of compound **8** in the smectic C* mesophase.

3.3 Electro-optic investigations

The switching behavior of the olefinic precursor **5**, heptamethyltrisiloxane substituted derivative **6** and the dimer **8** with two identical calamitic mesogens connected by a disiloxane spacer have been investigated by the electro-optical studies in the temperature range of chiral tilted smectic phase (SmC*). Electro-optical investigations were carried out in 10 µm polyimide (PI) coated indium tin oxide (ITO) cell. The samples were filled into cell in their isotropic phase through capillary action and cooled slowly to the temperature range of SmC* mesophase. AC triangular-wave voltage was applied of up to 340 Vpp. A small single polarization current peak was detected under an applied triangular wave voltage between 180°C and 100 °C for compound **5** and **8** (see Fig. 10a,b and 10e,f). In the temperature range of SmC* mesophase of compounds **6**, a single sharp polarization current peak in each half period of an applied triangular wave field was observed in the switching current curves indicating a ferroelectric switching behaviour (see Fig. 10c,d). From these observations one can infer that there are significant ferroelectric interactions between the mesogens **6** in the adjacent layers which bulky siloxane moieties tend to aggregate as compared to olefinic precursor **5** and dimer-structured molecule **8**. The result of quantitative analysis by integrating the area under the peaks reveals a polarization value (P_S) of around 200 nC cm^{-2} for compounds **5**, **6** and **8**. This case is in line with the switching behaviour and polarization value obtained in the SmC* phase of previously reported olefinic precursor and siloxane substituted derivatives with a chiral moiety[22] The switching current response obtained under a triangular wave field at 176.0 °C, 181.0 °C and 177.0 °C and the optical texture of the SmC* mesophase obtained under the same experimental conditions for compounds **5**, **6** and **8**, respectively, are shown in Fig. 10.

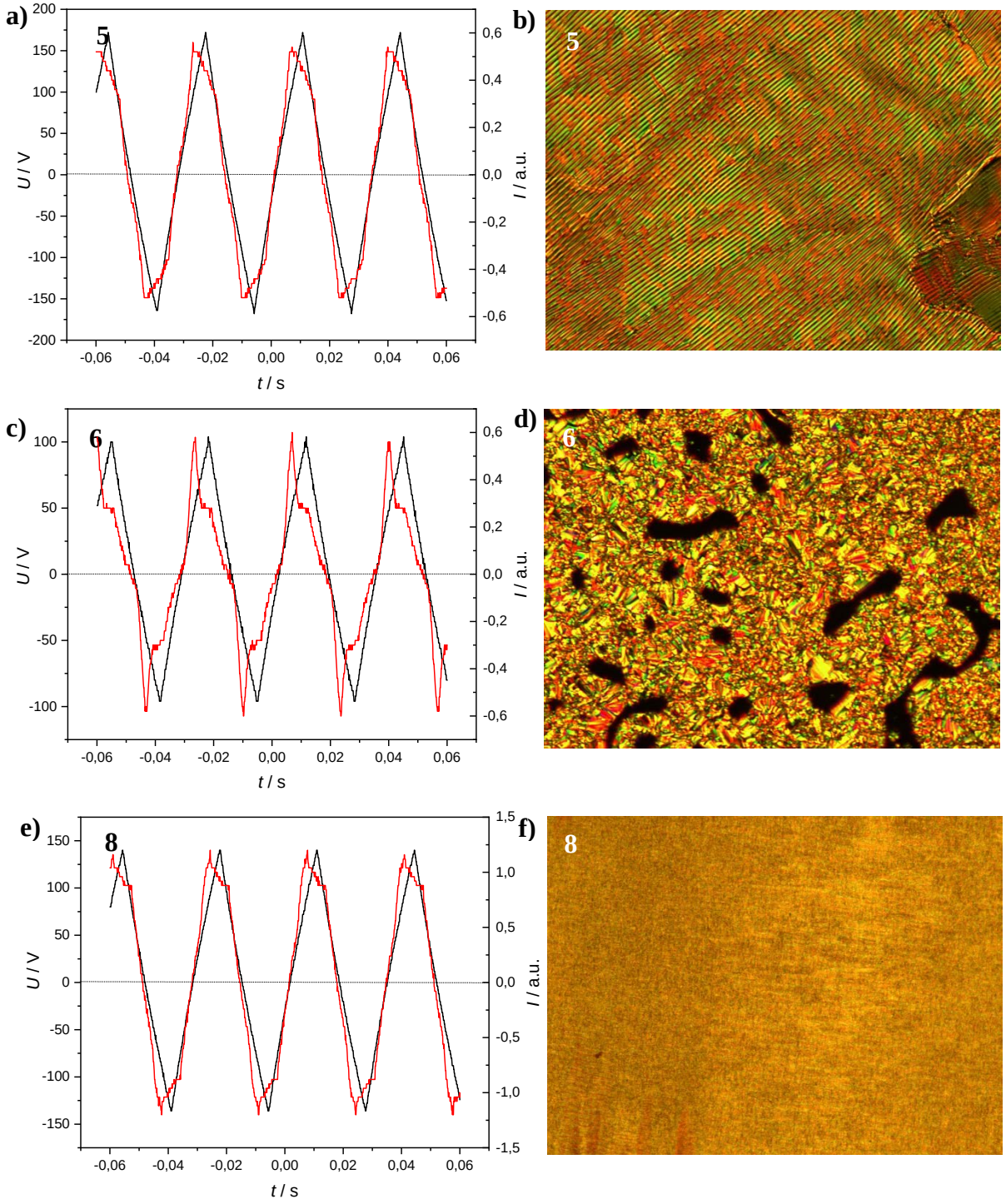

Fig. 10. (a,c,e) Switching current response obtained for compounds **5**, **6** and **8** in a 10 μm PI coated ITO cell under a triangular wave field and (b, d, f) the texture observed under these conditions, (a and b) at T = 176 °C, 340 Vpp, 30 Hz, 5 kΩ, P_S = 248 nC cm^{-2}; (c and d) at T = 181 °C, 200 Vpp, 30 Hz, 5 kΩ, P_S = 195 nC cm^{-2} and (e and f) at T = 177 °C, 280 Vpp, 100 Hz, 5 kΩ, P_S = 238 nC cm^{-2}.

4. Conclusion

In this study, new biphenyl based chiral calamitic mesogens bearing a (*S*)-2-methylbutoxy chiral moiety at one side and a siloxane end chain on the other side have been designed and synthesized in order to investigate the effect of combining the chiral moiety and siloxane segments within the same structure. Additionally, a dimer with the two identical chiral calamitics linked by a disiloxane spacer have been obtained via hydrosilylation reaction. The mesomorphic characterization shows that all target compounds exhibit enantiotropic chiral mesophases such as chiral tilted smectic phase (SmC*) and chiral nematic phase (N*). The introduction of 1*H*-heptamethyltrisiloxane end-group to the vinyl-terminated calamitic compound exhibiting enantiotropic chiral nematic phase (N*) and chiral tilted smectic phase (SmC*) leads to the suppression of the chiral nematic phase (N*) in the siloxane derivative and conduct to the formation of more stable chiral tilted smectic phase (SmC*) with lower clearing point. The incorporation of 1*H*,3*H*-tetramethyldisiloxane fragment simply induces a slight contraction of the lamellar period without affecting the domain of existence of the SmC*. Similar to the mesomorphic behaviour of olefinic precursor, the dimer with two identical calamitic mesogens connected by a disiloxane spacer exhibited a wider smectic mesophase interval in addition to the presence of N* mesophase was preserved. The electro-optic studies show that new mesogens with a chiral moiety exhibit a ferroelectric switching in their SmC* mesophase interval with the polarization values (P_S) of around 200 nC cm^{-2}.

Acknowledgement

This research has been supported by Yildiz Technical University Scientific Research Projects Coordination Department. Project Number: 2011-01-02-YULAP06. The authors are grateful to the TÜBİTAK-2232 Programme for a support with Project Number 118C273. B.B.E. and H.O. are grateful to the Alexander von Humboldt Foundation for financial support toward LC research. F.C. and O.J. also thank the Institut des Sciences Chimiques de Rennes, the University of Rennes 1 and Rennes Metropole for their financial support.

Appendix A. Supplementary data

Electronic supplementary information (ESI) available.

References

[1] C. Tschierske, Development of structural complexity by liquid crystal self-assembly, Angew. Chem. Int. Ed. 52 (2013) 8828-8878.

[2] M. Kohout, A. Bubnov, J. Šturala, V. Novotná, J. Svoboda, Effect of alkyl chain length in the terminal ester group on mesomorphic properties of new chiral lactic acid derivatives, Liq. Cryst. 43 (2016) 1472-1475.

[3] M. Lehmann, G. Kestemont, R. G. Aspe, C. Buess-Herman, M. H. J. Koch, M. G. Debije, J. Piris, M. P. De Haas, J. M. Warman, M. D. Watson, V. Lemaur, J. Cornil, Y. H. Geerts, R. Gearba, D. A. Ivanov, High charge-carrier mobility in π-deficient discotic mesogens: design and structure-property relationship, Chem. A. Eur. J. 11 (2005) 3349-3362.

[4] M. O'Neill and S. M. Kelly, Liquid Crystals for charge transport, luminescence, and photonics, Adv. Mater. 15 (2003) 1135-1146.

[5] C. E. Girotto, I. H. Bechtold, H. Gallardo, New liquid crystals derived from thiophene connected to the 1,2,4-oxadiazole heterocycle, Liq. Cryst. 12 (2016) 1768-1777.

[6] T. Ghosh, M. Lehmann, Recent advances in heterocycle-based metal-free calamitics, J. Mater. Chem. C 5 (2017) 12308-12337.

[7] T. Matsumoto, A. Fukuda, M. Johno, Y. Motoyama, T. Yui, S.-S. Seomunc, M. Yamashita, A novel property caused by frustration between ferroelectricity and antiferroelectricity and its application to liquid crystal displays-frustoelectricity and V-shaped switching, J. Mater. Chem., 9 (1999) 2051-2080.

[8] A. Liu, Q. Sun, J. Cui, J. Zheng, W. Liu, X. Wan, Tuning mesomorphic properties and handedness of chiral calamitic liquid crystals by minimal modification of the effective core, Chirality 23 (2011) E74-E83.

[9] G. Galli, B. Saliva, A. Lotz, L. Komitov, G. Scherowsky, E. Chiellini, New monomer liquid crystals containing a chiral 2,2- or 2,3-disubstituted oxirane ring, Designed Monomers and Polymers 3(4) (2000) 463-477.

[10] C.T. Liao, J. Y. Lee, C. C. Lai, A study of the wide ferroelectric phase in mixtures of chiral and non-chiral tilted smectic C-type liquid crystals, Material Chemistry and Physics 125(3) (2010) 749-756.

[11] J. P. F. Lagerwall, F. Giesselmann, Current topics in smectic liquid crystal research, ChemPhysChem. 7 (2006) 20-45.

[12] P. Rudquist, T. Carlsson, L. Komitov, S. T. Lagerwall, The flexoelectro-optic effect in cholesterics, Liq. Cryst. 22 (1997) 445-449.

[13] P. Rudquist, L. Komitov, S. T. Lagerwall, The flexoelectrooptic effect, Ferroelectrics 213 (1998) 53-62.

[14] H. Ocak, B. Bilgin-Eran, C. Tschierske, U. Baumeister, G. Pelzl, Effect of fluorocarbon chains on the mesomorphic properties of chiral imines and their complexes with copper(II), J. Mater. Chem. 19 (2009) 6995-7001.

[15] Y. Nagashima, T. Ichihashi, K. Noguchi, M. Iwamoto, Y. Aoki, H. Nohira, The synthesis and mesomorphic properties of ferroelectric liquid crystals with a fluorinated asymmetric frame, Liq. Cryst. 23 (1997) 537-546.

[16] J. Hemine, A. Daoudi, C. Legrand, A. El kaaouachi, A. Nafidi, M. Ismaili, N. Isaert, H.T. Nguyen, Electro-optic and dynamic studies of biphenyl benzoate ferroelectric liquid crystals, Physica B 405 (2010) 2151-2156.

[17] Y. Chen, W.-J. Wu, Synthesis and characterization of new ferroelectric liquid crystals containing oligomethylene spacers, Liq. Cryst. 25 (1998) 309-318.

[18] R. Asep, O. Aoki, T. Hirose, H. Nohira, Synthesis and physical properties of laterally fluoro substituted ferroelectric liquid crystals with a fluoro substituted chiral terminal chain, Liq. Cryst. 28 (2001) 785-791.

[19] C. Carboni, A. K. George, W. M. Zoghaib, The electro-optic response in a series of chiral bi-mesogen low molar mass organosiloxane liquid-crystal materials, Mol. Cryst. Liq. Cryst. 546 (2011) 215-220.

[20] L. Li, C. D. Jones, J. Magolan, R. P. Lemieux, Siloxane-terminated phenylpyrimidine liquid crystal hosts, J. Mater. Chem. 17 (2007) 2313-2318.

[21] J. C. Roberts, N. Kapernaum, F. Giesselmann, M. D. Wand, R. P. Lemieux, Fast switching organosiloxane ferroelectric liquid crystals, J. Mater. Chem. 18 (2008) 5301-5306.

[22] D. R. Medeiros, M. A. Hale, R. J. P. Hung, J. K. Leitko, C. G. Willson, Ferroelectric cyclic oligosiloxane liquid crystals, J. Mater. Chem. 9 (1999) 1453-1460.

[23] N. Olsson, M. Schröder, S. Diele, G. Andersson, I. Dahl, B. Helgee, L. Komitov, A new series of liquid crystalline dimers with exceptionally high apparent tilt, J. Mater. Chem. 17(24) (2007) 2517-2525.

[24] D. Guillon, M. A. Osipov, S. Méry, M. Siffert, J.-F. Nicoud, C. Bourgogne, P. Sebastião, Synclinic-Anticlinic Phase Transition in Tilted Organosiloxane Liquid Crystals, J. Mater. Chem. 11 (2011) 2700-2708.

[25] Y. Zhang, U. Baumeister, C. Tschierske, M. J. O'Callaghan, C. Walker, Achiral bent-core molecules with a series of linear or branched carbosilane termini: dark conglomerate phases, supramolecular chirality and macroscopic polar order, Chem. Mater. 22 (2010) 2869-2884.

[26] H. J. Coles, M. J. Clarke, S. M. Morris, B. J. Broughton, A. E. Blatch, Strong flexoelectric behavior in bimesogenic liquid crystals, J. Appl. Phys. 99 (2006) 034104-034107.

[27] G. Shanker, M. Prehm, C. Tschierske, Laterally connected bent-core dimers and bent-core-rod couples with nematic liquid crystalline phases, J. Mater. Chem. 22 (2012) 168-174.

[28] B. Kosata, G. M. Tamba, U. Baumeister, K. Pelz, S. Diele, G. Pelzl, G. Galli, S. Samaritani, E. V. Agina, N. I. Boiko, V. P. Shibaev, W. Weissflog, Liquid-Crystalline Dimers Composed of Bent-Core Mesogenic Unit, Chem. Mater. 18 (2006) 691-701.

[29] G. Shanker, M. Prehm, M. Nagaraj, J. K. Vij, C. Tschierske, Development of polar order in a bent-core liquid crystal with a new sequence of two orthogonal smectic and an adjacent nematic phase, J. Mater. Chem., 21 (2011) 18711-18714.

[30] H. Ocak, B. Bilgin-Eran, M. Prehm, C. Tschierske, Effects of molecular chirality on superstructural chirality in liquid crystalline dark conglomerate phases Soft Matter 8 (2012) 7773-7783.

[31] F. T. Niesel, J. Springer, S. Czapla, D. Wolff, J. Rübner, Phase transitions of side-group liquid crystalline polymers with a metastable S_A phase, Macromol. Rapid Commun. 15(1) (1994) 7-13.

[32] J.-S. Hu, B.-Y. Zhang, A.-J. Zhou, B.-G. Du and L.-Q. Yang, Synthesis and mesomorphic properties of a new side-chain, chiral smectic, liquid-crystalline elastomer, J. Appl. Polym. Sci. 100 (5) (2006) 4234-4239.

[33] B. Otterholm, M. Nilsson, S. T. Lagerwall, K. Skarp, Properties of some broad band chiral smectic C materials, Liq. Cryst. 2 (1987) 757-768.

[34] C. Tschierske, H. Zaschke, A mild and convenient esterification of sensitive carboxylic acids, J. Prakt. Chem. 331 (1989) 365-366.

[35] K. Fodor-Csorba, A. Vajda, A. Jakli, C. Slugovc, G. Trimmel, D. Demus, E. Gacs-Baitz, S. Hollye, G. Gallif, Ester type banana-shaped liquid crystalline monomers: synthesis and physical properties, J. Mater. Chem. 14 (2004) 2499-2506.

[36] C. Keith, R. A. Reddy, A. Hauser, U. Baumeister, C. Tschierske, Silicon-Containing Polyphilic Bent-Core Molecules: The Importance of Nanosegregation for the Development of Chirality and Polar Order in Liquid Crystalline Phases Formed by Achiral Molecules, J. Am. Chem. Soc. 128 (2006) 3051-3066.

[37] G. H. Mehl, J. W. Goodby, Supermolecules Containing a Tetrahedral Core: A New Class of Liquid-Crystalline Siloxanes, Chem. Ber. 129 (1996) 521-525.

[38] J. Newton, H. J. Coles, H. Owen, P. Hodge, A new series of low molar mass ferroelectric organosiloxanes with unusual electro-optic properties, Ferroelectrics 148 (1993) 379-387.

[39] T. Hanasaki, Y. Kamei, A. Mandai, K. Uno, K. Kaneko, The phase transition behaviour and electro-rheological effect of liquid crystalline siloxane dimers, Liq. Cryst. 38 (7) (2011) 841-848.

[40] W. K. Robinson, C. Carboni, P. Kloess, S. P. Perkins, H. J. Coles, Ferroelectric and antiferroelectric low molar mass organosiloxane liquid crystals, Liq. Cryst. 25 (1998) 301-307.